Paper presented at:

13th Personal Armour Systems Symposium - PASS 2016.
19-23 September 2016. Amsterdam (Netherlands)

GOBIERNO DE ESPAÑA
MINISTERIO DE ECONOMÍA, INDUSTRIA Y COMPETITIVIDAD

UNIÓN EUROPEA
FONDO EUROPEO DE DESARROLLO REGIONAL
"Una manera de hacer Europa"

UNIÓN EUROPEA
FONDO EUROPEO DE DESARROLLO REGIONAL
"Una manera de hacer Europa"

Project RTC-2015-3887-8

Behavior of a new combat helmet design against ballistic impact: Experimental and numerical analysis.

M. Rodríguez-Millán[1], A. Olmedo[2], G. Romualdo[2], N.Feito[1], J.A. Loya[3] and M.H. Miguélez[1]

[1]*Department of Mechanical Engineering, University Carlos III of Madrid, Avda. de la Universidad 30, 28911 Leganés, Madrid, Spain*
mrmillan@ing.uc3m.es

[2]*FECSA S.A, c. de Acacias 3, 28703 San Sebastián de los Reyes, Madrid, Spain*
aolmedo@fecsa.net

[3]*Department of Continuum Mechanics and Structural Analysis, University Carlos III of Madrid, Avda. de la Universidad 30, 28911 Leganés, Madrid, Spain*

Abstract.

This work focuses on the finite element analysis (FEA) of a new combat helmet design developed by the Spanish Company FECSA S.A. with the aim of optimizing the final design. The helmet was made of aramid/phenolic resin. Mechanical behavior under impact conditions were analyzed through the experimental Fragment Simulating Projectile (FSP) and Full-Metal Jacketed (FMJ) impact tests on aramid flat plates. From this point, the helmet numerical model, developed using the commercial code ABAQUS/Explicit, was optimized in order to reach the required ballistic limit. Since the aramid composite mechanical properties depends on fiber orientation, a user-defined subroutine VUMAT was developed to simulate the composite behavior under ballistic penetration. For the final validation of the proposed numerical model, experimental impact tests on helmets were performed showing good agreement with the numerical predictions.

1. INTRODUCTION

Given the recent rise in terrorism, civil and international conflicts, the number of people afflicted with war-related traumatic brain injuries (TBI) is set to increase. In this sense, TBI is most often related to their exposure to blast and ballistic threats, such as those from shrapnel, shell fragments, and bullets.

In order to minimize the morbidity and mortality resulting from ballistic head injuries, it is particularly important to ensure that personal protective equipment, especially the combat helmets, are capable and effective in providing protection from ballistic impact. However, even using a proper helmet, other serious injuries can be emerged such as behind helmet blunt trauma (BHBT). This trauma is due to non-penetrating ballistic impacts and is often associated with helmet back face deformation (BFD) [1]. Several works have focused on analyzing this effect [2-7].

Combat helmets have evolved considerably over the years: the first generations of helmet were made of steel advancing to the current generations in general based on aramid composites [8]. The most common aramid composite, Kevlar®, presents excellent properties as high strength, high modulus, and high strength-to-weight ratio. The large scale deformation of the yarns offers penetration resistance against incident high energy projectiles [9].

Innovative helmet designs require testing of structural elements constituting the personal protection. In order to reach proper protection, manufacturers subject the helmet to series of ballistic tests. Ballistic impact tests used by manufacturers are defined in NIJ STANDARD 0106.01 for ballistic helmets [10] and STANDARDIZATION AGREEMENT (STANAG) 2920: Ballistic Test Method for personal armor materials and combat clothing. These standards are the most used by the manufacturers [11].

STANAG 2920 [11] uses chisel-nosed fragment-simulating projectiles for proof-testing. The 1.1 g (17 grain) fragment simulating projectile (FSP) with 0.22-caliber (5.5mm diameter) is most commonly

used. This standard is used to calculate V_{50} of a specimen, which is defined as a striking velocity for which there exist a 50% probability of perforation of the barrier or some protective device [12]. In the simplest approach, V_{50} could be determined by averaging six projectile-striking velocities that include three lowest velocities that resulted in complete penetration and the three highest velocities that resulted in a partial penetration [13].

NIJ-STD-0106.01[10] establishes performance requirements and methods of testing helmets intended to protect the wearer against gunfire. The standard classifies ballistic helmets into three types by the level of performance. This study focuses on Type II which establishes ballistic impact performance requirements for a helmet when impacted by a 9 mm full-metal jacketed (FMJ) bullet weighing 8g (124 grain) from the front, side, rear and top of the combat helmet at 425 ± 15m/s. A pad system and headform with Roma Plastilina No 1 are used to measure the helmet back face deformation. The helmet pad used was the Oregon Aero interior foam cushioning system.

Despite the importance of carrying out experimental tests, specimens are difficult to obtain, and testing can be lengthy and expensive. In this sense, numerical modeling provides an interesting tool for characterizing the physics of the problem in terms of relevant mechanical variables such as stress, strain, and acceleration. Therefore, numerical models can be used as a virtual testing tool in order to optimize materials and designs against different situations.

The objective of this work was to develop a numerical finite element model able to determine the response of a new combat helmet, developed by FECSA, subjected to ballistic impact. Experimental tests on plates were performed in order to obtain material properties and to calibrate the numerical model. Predicted results for the designed helmet under ballistic impact will be compared with real impact tests showing the accuracy of the model and its ability to be used as an optimizing design tool.

2. BALLISTIC BEHAVIOUR OF ARAMID PLATES

Experimental tests were carried out according to standards described above with the objective of analyzing the mechanical behaviour of the aramid composite under ballistic impact. A numerical model has been developed and calibrated with these experimental tests. This model will be used to further simulate the combat helmet in order to predict the efficiency of the helmet under ballistic impacts.

The dimensions of aramid composite specimens considered are 400 x 400 mm with areal density 8.86 kg/m^2. The aramid composite specimens contain more than 20 laminate layers and are molded with Kevlar 29/polyvinyl butyral-phenolic composite. The specimens were made by a compression molding process

2.1. Numerical Model

The model was developed using the finite element (FE) commercial code ABAQUS/Explicit based on a Lagrangian approach, allowing efficient reproduction of the dynamic loading processes. The contact between the projectiles and the plates was defined with a penalty contact algorithm and hard contact model according to ABAQUS code user manual [14]. The ‘‘hard contact’’ option allows automatic adjustment of the stiffness, generated by the ‘‘penalty contact algorithm’’, to minimize penetration without adversely affecting the time increment.

Concerning frictional effects, it is assumed a dynamic frictional coefficient μ equal to 0.3 between steel and composite. Additionally, the coefficient of friction between the metal and Roma Plastilina No. 1 was 0.193 according to [22].

The details of the FE model are described in the following paragraphs:

2.1.1 Aramid composite plates

Target plates were meshed with C3D6 elements (6-node linear triangular prism) [14] with an element size of 4 mm. The FE model of the plates is simplified to just 4 layers to reduce computational cost and increase computational efficiency [15].

The behaviour of the aramid composite was modelled through the introduction of a user subroutine VUMAT assuming elastic behaviour up to failure. Failure was predicted using the Hashin failure criteria [16] implemented in a VUMAT user subroutine [15] (parameters presented in Table 1). Numerous studies on low and high-velocity impact have demonstrated the accuracy of Hashin failure criteria to model the dynamic behaviour of woven composites, see for example [13,15,17].

Table 1. Failure properties of aramid composite [15,18].

$X1_T$ (MPa)	$X1_C$ (MPa)	$X2_T$ (MPa)	$X2_C$ (MPa)	$X3_T$ (MPa)	$X3_C$ (MPa)	S_{12} (MPa)	S_{13} (MPa)	S_{23} (MPa)
555	555	555	555	1050	1050	77	1060	1086

2.1.2 Fragment Simulating Projectile (FSP)

The projectile used in the simulation is a 1.1 g FSP based on STANAG 2920[11] which is made of AISI 4340. The FSP was meshed with C3D6 elements and average size 0.3 mm, Figure 1.

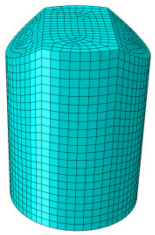

Figure 1. Numerical model of Fragment Simulating Projectile (FSP).

The thermo-viscoplastic material behaviour of the FSP material is defined using the Johnson-Cook (JC) model [19]. The JC model is generally pre-implemented in finite element (FE) codes, including ABAQUS/explicit.

For AISI 4340, the parameters of the constitutive equation were obtained from Ozel, et.al. [20] and are shown in Table 2 together with other physical properties.

Table 2. Mechanical properties of AISI 4340 [20].

Elasticity			**Thermo-viscoplastic behaviour**					
$E(GPa)$	$\nu(-)$		$A(MPa)$	$B(MPa)$	$n(-)$	$\dot{\varepsilon}_0(s^{-1})$	$C(-)$	$m(-)$
210	0.3		792	510	0.34	1	0.014	1.03
Other physical constants								
$\rho(kg/m^3)$		$\beta(-)$	$C_p(J/kg\,K)$		$T_0(K)$		$T_m(K)$	
2700		0.9	477		293		1793	

Moreover, the model took into account the relationship between pressure, mass-density, and internal-energy density/temperature by Mie–Gruneisen EOS. The material parameters of EOS are taken from [14], Table 3.

Table 3. Material parameters of EOS [14].

$C_0(m/s)$	S_α	Γ_0
3935	1.578	1.69

2.1.3 Full Metal Jacket (FMJ) Bullet.

The dimensions and FE mesh of a 9 mm FMJ bullet, weighing about 8 g, are shown in Figure 2. The dimensions are specified according to the STANAG 4090 Ed.2 [10]. The bullet has two components: a copper jacket and a lead core. Seven hundred and fifty-two hexahedral elements are used in discretizing the FMJ bullet. The copper jacket material is further modeled by the Johnson Cook

model and damage initiation criterion (Table 4) while the lead material is assumed as elastic with EOS (Table 5) [21].

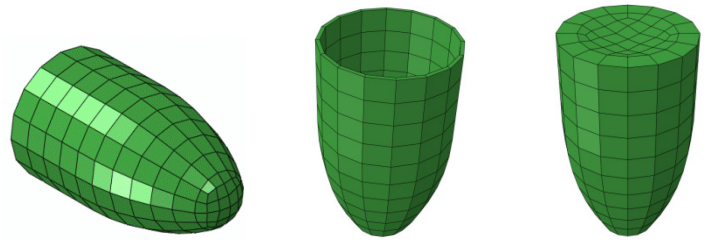

a) b) c)

Figure 2. Numerical model of a) Full Metal Jacket (FMJ); b) cartridge brass and c) lead core

Table 4. Mechanical properties of cartridge brass [21].

Elasticity		**Thermo-viscoplastic behaviour**					
$E(GPa)$	$\nu(-)$	$A(MPa)$	$B(MPa)$	$n(-)$	$\dot{\varepsilon}_0(s^{-1})$	$C(-)$	$m(-)$
210	0.3	112	505	0.42	1	0.009	1.68
		Johnson Cook Damage					
		D_1		D_2	D_3	D_4	D_5
		0.54		4.89	0.014	3.03	1.12
Other physical constants							
$\rho(kg/m^3)$	$\beta(-)$	$C_p(J/kg\,K)$		$T_0(K)$		$T_m(K)$	
2700	0.9	477		293		1793	

Table 5. Mechanical properties of lead core [21].

$\rho(kg/m^3)$	$E\ (MPa)$	$C_0(cm/\mu s)$	S_α	Γ_0
11840	200	3935	1.429	2.60

2.1.4 Roma Plastilina No.1.

The material used in this work is a commercially available soft Roma Plastilina No. 1 clay, colour grey-green. The mechanical behaviour has been modelled based on the Ludwik constitutive relation (Equation 3) according to [22].

$$\bar{\sigma} = k(\bar{\varepsilon}^p)^n \left(\frac{\dot{\bar{\varepsilon}}^p}{\dot{\bar{\varepsilon}}_0}\right)^m \tag{3}$$

where k is the material constant, n is the strain hardening coefficient, m is the strain rate sensitivity coefficient and $\dot{\bar{\varepsilon}}_0$ is the initial strain rate usually set to 1. The material properties are listed in Table 6 [22, 23].

Table 6. Mechanical properties of Roma Plastilina No. 1

$\rho(kg/m^3)$	$E\ (MPa)$	$\nu(-)$
1529	4.92	0.49

2.2 Experimental tests on plates

Seven shots have been conducted with 1.1 g FSP based on STANAG 2920 with a velocity of 650 ± 40 m/s. The Spanish Military Standard NME-2786 [24] establishes that the V_{50} must be equal to or higher than 650 m/s for all tests. The result of V_{50} after seven shots (Table 7) was 687 m/s for aramid composite plates, this value was higher than that obtained by other researchers for aramid composite plates (586 m/s [25], 610 m/s [14]) and more similar to the 680 m/s obtained by Colakoglu *et al.* [26]. The differences between our result and the others may due to differences in the experimental set up. The Figure 3 shows the final stage of the penetration for the front and back side

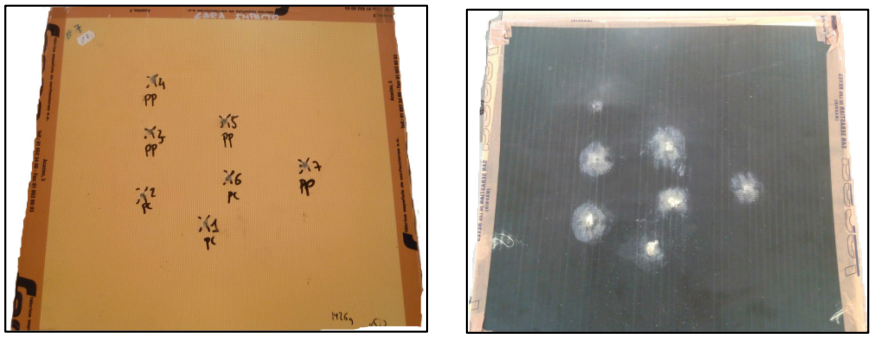

a) b)

Figure 3. Final stage of the STANAG 2920 tests for seven shots. a) Front and b) back sides.

In accordance with NIJ-STD-0106.01 protocol, seven shots were conducted with 9 mm full metal jacket (FMJ) bullet, with nominal mass of 8.0 g (124 grain) and velocity of 425 ± 15 m/s. Figure 4 shows the final stage of the penetration for front and back side.

a) b)

Figure 4. Final stage of the test conducted using NIJ STANDARD 0106.01 protocol for seven shots. a) front and b) back sides.

2.3 Calibration and validation of the numerical model

In order to optimize the numerical model for the aramid composite under ballistic impact, experimental results have been used for comparison.

The numerical process of the impact is shown in Figure 5 for an interval of 0-50 μs. It can be observed that the FSP moved very little from *t=40 μs*. This is consistent with the impact velocity evolution of the FSP (Figure 6) and with the experimental result of V_{50}.

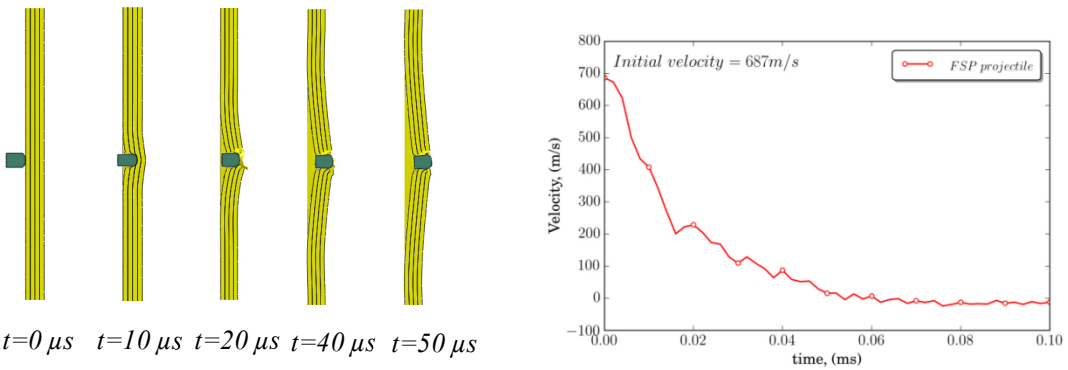

Figure 5. Evolution of the impact process for aramid composite plates using STANAG 2920 protocol. Initial velocity= 697 m/s.

In order to calibrate and validate the numerical model, more experimental tests were performed. The experimental tests were carried out using spherical projectiles of diameter 7.5 mm. The table 7 shows the data obtained.

Table 7. Validation of numerical model for impact tests using spherical projectiles.

NºTest	$V_0(m/s)$	$V_r^{exp}(m/s)$	$V_r^{num}(m/s)$
3	537	0	0
4	579	0	0
6	593	167	165
5	612	240	186
8	650	332	338
7	661	385	385
2	693	469	469
1	782	563	540

The NIJ-STD-0106.01 was taken into account for the other calibration. An evolution of impact process by numerical simulations is shown in Figure 6.

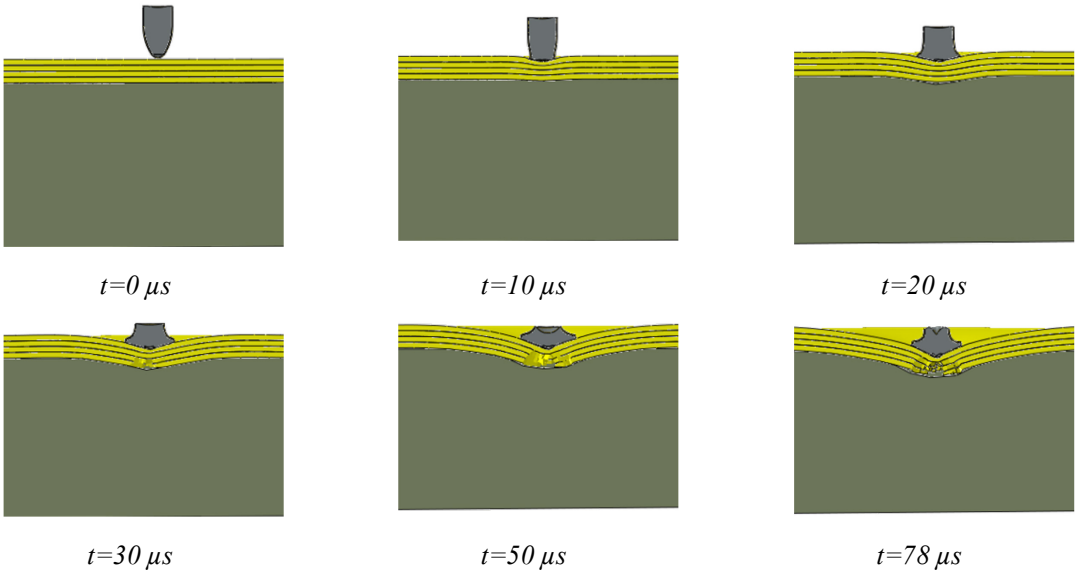

Figure 6. Evolution of the impact process for aramid composite plates using NIJ-STD-0106 protocol. The initial impact velocity= 425 m/s.

The values of Back Face Deformation (BFD) obtained can be summarized in Table 8 for impact velocity V_0=425 m/s. The experimental BFD obtained was 21.8 ± 1.35 mm while the numerical one was 20 mm. These values are similar to BFD obtained by Colakoglu *et al.* [26], 21.6 mm. The difference between our values and those in the literature was due to aramid composite used in [26]. Those were 9.28 kg/m^2 while the plates in this study were 8.86 kg/m^2. The experimental BFDs increased because the impact tests were sequential and the plate damage also increased.

Table 8. Comparison of Back Face Deformation (BFD) for aramid composite plates.

Nº Test	Experimental (mm)	Numerical (mm)	Colakoglu *et al.* [25]
1	18	20	21.6
2	20		
3	22		
4	23		

5	26		
Average	21.8 ± 1.35		

3. BALLISTICS TESTS ON COMBAT HELMETS

Once the mechanical behavior of the aramid composite was calibrated with impact on flat panels, a numerical model for a combat helmet was developed and compared with the experimental tests on combat helmets in order to obtain the V_{50} velocity.

3.1. Numerical combat helmet model

The combat helmets were subjected to impacts with FSP projectiles according to STANAG 2920 (aramid model and FSP described in section 2.1). So, the proper combat helmet and interior foams have been considered.

3.1.1 Combat helmet

A new combat helmet shell was developed by the Spanish company FECSA (Figure 7 a) using a compression molding process. The FE helmet model (Figure 11 b) was modelled with 4 layers as the plates described in section 2.1.

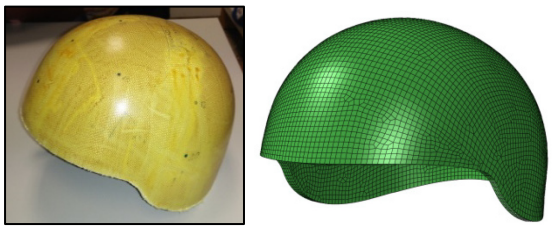

Figure 7. a) New combat helmet shell developed by the Spanish company FECSA; b) Numerical model of shell combat helmet.

3.1.2 Interior foams

The interior foams were modelled using the Low Density Foam material model available in ABAQUS which is intended for low-density, highly compressible elastomeric foams with significant rate sensitive behaviour, such as polyurethane foam. The model requires as input, the stress-strain response of the material for both uniaxial tension and uniaxial compression tests. Rate-dependent behaviour is specified by providing the uniaxial stress-strain curves for different values of nominal strain rates [14]. The mechanical behaviour of the Oregon Aero (OA) foam padding is obtained from literature [15] assuming that it is a homogenous material. The mesh of foams was 105628 hexaedral C3D8R with average size 4 mm, Figure 8.

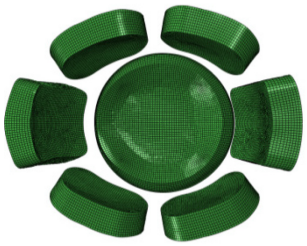

Figure 8. Numerical model of Oregon Aero (OA) foam.

3.2 Validation of numerical model with experimental tests on combat helmet

Eight shots in a wide range of impact velocities ($663.6\ m/s \leq V_0 \leq 732\ m/s$) (Table 9) in different places of the helmet were performed (Figure 9), resulting in an experimental V_{50} of 697 m/s (higher than calculated by other researchers [14, 27, 28]).

a) Frontal b) Top c) Rear

c) Right side d) Left side

Figure 9. Final stage of the STANAG 2920 tests on combat helmets

The numerical process of the impact is shown in Figure 10 where the FSP is stopped by combat helmet shell for a V_{50}=697 m/s. Detail of the final stage of the impact process can be observed in the Figure 11.

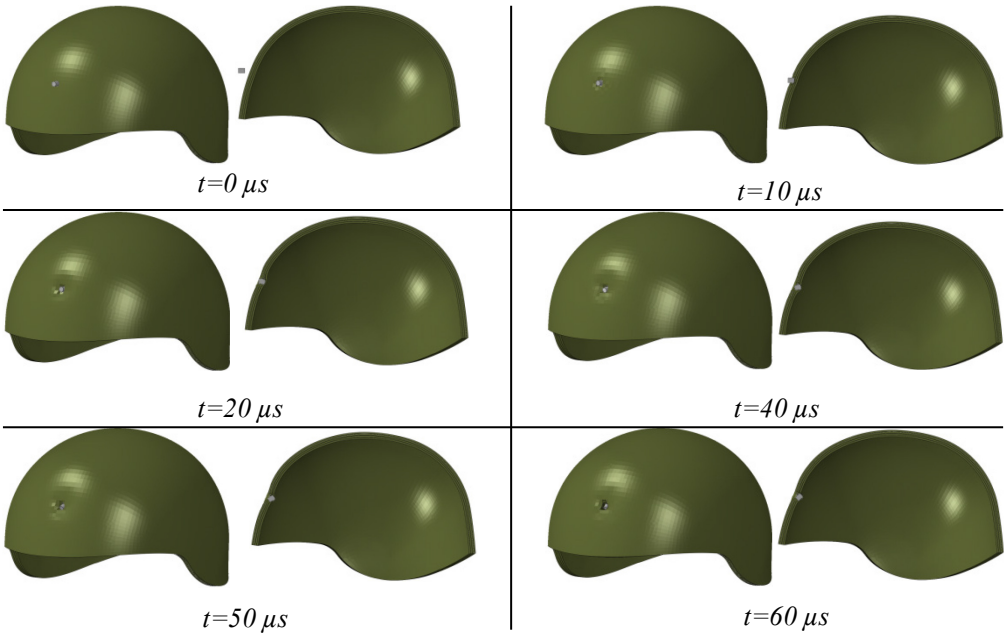

Figure 10. Evolution of impact process on combat helmets using the STANAG 2920 protocol with an initial impact velocity= 697 m/s.

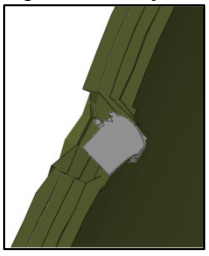

Figure 11. Detail of Final stage of the impact process on combat helmets using the STANAG 2920 protocol.

Table 9. Experimental and numerical tests in order to obtain the V50 velocity.

Impact Velocity (m/s)	**Experimental results**	**Numerical results**
	Perforation	**Residual velocity** (m/s)
663.6	Partial	-
683.2	Partial	-
689.7	Partial	-
697.0	Partial	-
701.1	Complete	Very low (~ 0)
701.7	Complete	Very low (~ 0)
718.5	Complete	20
732.0	Complete	177

In order to clarify; the evolution of FSP with time, data have been plotted in the Figure 13. In this figure, the bullet kept moving on until *t=0.08 ms*.

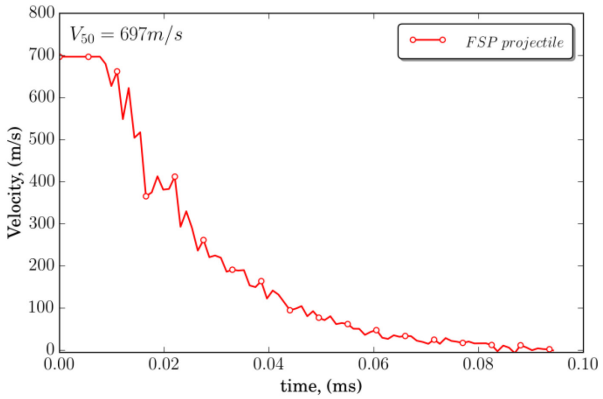

Figure 13. Evolution of impact velocity on combat helmet using STANAG 2920 protocol. Case: front impact.

4. CONCLUSIONS

In this work, a finite element model has been used to optimize a new combat helmet developed by the Spanish Company FECSA S.A. The mechanical properties of the aramid composite have been calibrated from FSP and FMJ impact tests on aramid flat plates. These properties have been implemented in a complete numerical helmet model. The model may be considered in order to improve and optimize the combat helmet. The model has been used as a predictive tool to calculate the ballistic limit on the new combat helmet. The V_{50} velocity obtained was 697.0 m/s which is higher than values found in the literature for similar configurations. The results of this work have demonstrated that the helmet evaluated in this study has the potential to meet the requirements established by manufacturers for helmet performance against a specific set of ballistic treats.

Acknowledgments

The authors acknowledge the Ministry of Economy and Competitiveness of Spain under the Project RTC-2015-3887-8 for the financial support of the work.

References

[1] Li, Y. Q., Li, X. G. and Gao, X.-L., Modeling of Advanced Combat Helmet Under Ballistic Impact. J. Appl. Mech., 82(2015), 1110041-9.

[2] Carroll, A. W. and Soderstrom, C. A., A New Nonpenetrating Ballistic Injury, Ann. Surg., 188(1978), 753–757.

[3] Sarron, J.-C., Caillou, J.-P., Da Cunha, J., Allain, J.-C., and Tramecon, A., Consequences of Nonpenetrating Projectile Impact on a Protected Head: Study of Rear Effects of Protections, J. Trauma, 49(2000), 923–929.
[4] Cannon, L., Behind Armour Blunt Trauma—An Emerging Problem, J. R. Army Med. Corps, 147(2001), 87–96.
[5] Hisley, D. M., Gurganus, J. C. and Drysdale, A. W., Experimental Methodology Using Digital Image Correlation to Assess Ballistic Helmet Blunt Trauma, ASME J. Appl. Mech., 78(2011), 051022.
[6] Prat, N., Rongieras, F., Sarron, J.-C., Miras, A., and Voiglio, E., Contemporary Body Armor: Technical Data, Injuries, and Limits, Eur. J. Trauma Emergency Surg., 38(2012), 95–105.
[7] Freitas, C. J., Mathis, J. T., Scott, N., Bigger, R. P., and MacKiewicz, J., Dynamic Response due to Behind Helmet Blunt Trauma Measured With a Human Head Surrogate, Int. J. Med. Sci., 11(2014), 409–425.
[8] Council, N. R., Review of Department of Defense Test Protocols for Combat Helmets (2014).
[9] Termonia, Y., Impact resistance of woven fabrics, Textile Res. J. 84 (2004) 723–9.
[10] National Institute of Justice (NIJ) Standard, NILECJ-STD-0106.00: ballistic helmets, U.S.D.o. Justice, Washington, DC, US, (1975).
[11] Eriksen, J. H., STANAG 2920 Ed 2 Ballistic Test Method for Personal Armor Materials and Combat Clothing , 2nd ed. , NATO PfP (2003).
[12] Zukas JA, Nicholas T, Swift HF, Greszczuk LB and Curran DR., Impact Dynamics,Wiley, New York (1982).
[13] Tham, C. Y., Tan, V. B. C., and Lee, H. P., Ballistic impact of a KEVLAR® helmet: Experiment and simulations. Int. J. Impact Eng., 35(2008), 304–318.
[14] Dassault Systèmes. Abaqus v6.12 Documentation- ABAQUS analysis user's manual. ABAQUS Inc; 6.12 (2012).
[15] Tan, L. Bin, Tse, K. M., Lee, H. P., Tan, V. B. C. and Lim, S. P., Performance of an advanced combat helmet with different interior cushioning systems in ballistic impact: Experiments and finite element simulations. Int. J. Impact Eng. 50 (2012), 99–112.
[16] Hashin Z. Failure criteria for unidirectional fiber composites. Trans. ASME J. Appl. Mech. 47(1980), 329–34.
[17] Rodríguez-Millán, M., Moreno, C.E, Marco, M., Santiuste, C. and Miguélez, H., Numerical analysis of the ballistic behaviour of Kevlar composite under impact of double-nosed stepped cylindrical projectiles J Reinf. Plastics and Compos., 35 (2016), 124-137
[18] Gong, S.W., Lee, H.P. and Lu, C., Computational simulation of the human head response to non-contact impact. Comp. Struct.,86 (2008),758-70.
[19] Johnson, G.R. and Cook, WH., A constitutive model and data for metals subjected to large strains high strain rates and high temperatures. In: Proceedings of the seventh international symposium on ballistics (1983).
[20] Ozel T. and Zeren E., Finite element modeling the influence of edge roundness on the stress and temperature fields induced by high speed machining. Int. J. Adv. Manuf. Tech., 35(2007)255–267
[21] Tse, K. M., Development of a Realistic Finite Element Model of Human Head and its Applications to Head Injuries. PhD Dissertation: National University of Singapore, Department of Mechanical Engineering, (2013).
[22] Hernandez, C., Buchely, M.F. and Maranon, A., Dynamic characterization of Roma Plastilina No. 1 from Drop Test and inverse analysis. Int. J. Mech. Sci. 100 (2015) 158–168
[23] Sofuoglu, H. and Rasty, J., Flow behavior of Plasticine used in physical modeling of metal forming processes, Tribol. Int., Volume 33, Issue 8, August 2000, Pages 523-529]
[24] UNE-EN 960-2007 Cabezas de ensayo para utilizarse en los ensayos de cascos de protección. Marzo 2007.
[25] Van Hoof, J., Modelling impact induced delamination in composite materials. Ottawa: Carleton University; 1999.
[26] Colakoglu, M., Soykasap, O., Army, T., and Özek, T., Experimental and Numerical Investigations on the Ballistic Performance of Polymer Matrix Composites Used in Armor Design. Appl. Compos. Mater., 2(2007), 1–8.
[27] Cunniff PM., Decoupled response of textile body armor. In: Proceedings of the 18th international symposium on ballistics, San Antonio, TX, USA, (1999) 814–21.
[28] Lim, J. S. and Kim, J.H., Ballistic behavior of Heracron®-based composites: effect of fiber density and fabrication method, Compos. Interface, 21(6) (2014), 543–552.